X-ray study of metal-insulator transitions induced by W doping and photoirradiation in VO_2 films

D. Okuyama,[1,*] K. Shibuya,[1,2] R. Kumai,[3] T. Suzuki,[1] Y. Yamasaki,[1,3,4] H. Nakao,[3] Y. Murakami,[3] M. Kawasaki,[1,4] Y. Taguchi,[1] Y. Tokura,[1,4] and T. Arima[1,5]

[1]*RIKEN Center for Emergent Matter Science (CEMS), Wako 351-0198, Japan*

[2]*National Institute of Advanced Industrial Science and Technology (AIST), Tsukuba 305-8562, Japan*

[3]*Condensed Matter Research Center and Photon Factory, Institute of Materials Structure Science, KEK, Tsukuba, 305-0801, Japan*

[4]*Department of Applied Physics, University of Tokyo, Tokyo 113-8656, Japan*

[5]*Department of Advanced Materials Science, University of Tokyo, Kashiwa 277-8561, Japan*

(Received 18 September 2014; revised manuscript received 14 January 2015; published 3 February 2015)

A synchrotron x-ray diffraction study of metal-insulator transitions in W-doped VO_2 ($V_{1-x}W_xO_2$) thin films has been carried out. The insulating phase for $x \leqslant 0.07$ exhibits cell-doubling with the V dimerization similar to bulk VO_2, while the insulating phase for $x \geqslant 0.11$ does not. This result suggests that the electronic structure of the $x \geqslant 0.11$ insulators should be different from that of the $x \leqslant 0.07$ ones and bulk-insulating phase of VO_2. The temperature and x dependence of superlattice reflection as observed casts doubt about the direct relationship between the dimerization of V ions and metal-insulator transition. The temperature dependence of the electrical resistivity rather implies the Mott-Anderson localization nature of the insulating phases. X-ray-induced persistent phase transitions are observed at low temperatures in each insulating phase in the vicinity of the boundary to the metallic phase regardless of the difference in the electronic structure. Gradual peak shift suggests that the x-ray irradiation produces nanometer metallic regions.

DOI: 10.1103/PhysRevB.91.064101 PACS number(s): 71.30.+h, 73.61.−r, 61.05.cp

I. INTRODUCTION

Metal-insulator phase transitions accompanying structural deformation in strongly correlated electron systems have been extensively studied for decades [1,2]. VO_2 is well known to exhibit a first-order metal-insulator transition at ∼340 K. Because the nominal valence of V ions is 4+, the $3d$ band is partially occupied by one electron per V ion, giving rise to metallic conduction at high temperatures. At the metal-insulator transition temperature, the crystal structure simultaneously changes from tetragonal to monoclinic [3,4]. In this structural transition, V^{4+} ions are dimerized in each V chain along the c axis (M1 phase; see Fig. 1) [5,6]. The simultaneous transformation of the crystal and electronic structures results in a semiconducting transport property [7–12]. The effect of impurities on the metal-insulator transition has also been investigated by many researchers. It has been reported that Cr doping more than 1% modifies the pattern of V dimerization to form different types of monoclinic distortions (M2 and M3 phases) [13,14]. A minor amount of substitution of V by Nb, Mo, or W suppresses the metal-insulator transition temperature [15–18]. In the case of W doping, it has been suggested that the valence state of W is 6+, and that W acts as a donor [19,20]. Shibuya *et al.* fabricated single-crystalline thin films of W-doped VO_2 by using a pulse laser deposition (PLD) technique, and obtained the phase diagram of $V_{1-x}W_xO_2$ [21]. The metal-insulator transition temperature once decreases with increasing the W content for $x \leqslant 0.07$. The metallic ground state appears for $0.08 \leqslant x \leqslant 0.095$, where the collapse of a charge gap is observed in the optical conductivity spectra [22]. For $x \geqslant 0.11$, the metal-insulator transition revives and the transition temperature increases with increasing W content. Photoemission (PES) and x-ray absorption spectroscopies (XAS) were conducted to clarify the features of the two insulating phases [23]. The spectra for $x \leqslant 0.07$ is similar to that of VO_2 thin film while for $x \geqslant 0.11$, a temperature- and polarization-independent unoccupied $d_{\parallel}^*$ band appears above Fermi energy in XAS spectra, and the spectral weight transfer from a coherent peak at Fermi level to an incoherent peak is observed in PES. Based on the experimental results, it has been proposed that a Mott-Hubbard transition should take place for $x \geqslant 0.11$. If the origins of the metal-insulator transitions for $x \leqslant 0.07$ and for $x \geqslant 0.11$ are different as proposed, some clear difference in the structural property is expected. In this paper, the crystallographic aspects of the metal-insulator transition in W-doped VO_2 thin-film are investigated by means of synchrotron x-ray diffraction experiments. The V-dimerization and breaking of the glide symmetry in the M1 phase can be detected by an x-ray diffraction measurement. For example, in bulk VO_2, a structural phase transition from tetragonal $P4_2/mnm$ to monoclinic $P2_1/c$ with a jump of the c-axis length takes place upon the metal-insulator transition [4,13]. From the crystallographic aspects and the detailed analyses of the electric resistivity, we discuss the driving mechanism of the metal-insulator transition in W-doped VO_2 films.

VO_2-related materials have been attracting interest also from the viewpoint of photo-induced effects. A dynamical behavior of the photo-induced temporal structural change and electronic rearrangement was investigated by using femtosecond time-resolved x-ray diffraction and spectroscopy in VO_2 bulk material [24,25]. More recently, x-ray-induced persistent insulator-to-metal transition was observed in an $x = 0.065$ W-doped VO_2 thin film [26]. In the phase diagram of W-doped VO_2 thin film, two insulating phases compete with a metallic phase. One may thus expect that a large x-ray-induced effect could emerge in a wide x range [27,28].

*Present address: Institute of Multidisciplinary Research for Advanced Materials, Tohoku University, Katahira 2-1-1, Sendai 980-8577, Japan; okudaisu@tagen.tohoku.ac.jp

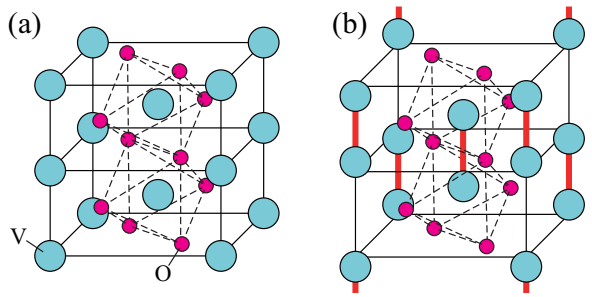

FIG. 1. (Color online) Schematic views of crystal structures of (a) metallic phase and (b) dimerized insulating phase in W-doped VO_2. Large (small) spheres indicate V (O) ions, respectively. Dotted lines represent octahedra of oxygen ions. Thick lines indicate V dimers.

We here report a systematic investigation of the x-ray-induced persistent insulator-metal transition. The mechanism of the photoirradiation-induced insulator-metal transition in W-doped VO_2 film is also investigated by detailed analyses of the temporal change of x-ray diffraction intensity.

II. EXPERIMENTAL

Thin films of $V_{1-x}W_xO_2$ with thicknesses of about 80 nm were fabricated on rutile-type TiO_2 (001)-substrates by a PLD method [21,26]. The epitaxial growth was confirmed by x-ray diffraction. The electrical resistivity was measured by a conventional four-probe method. Synchrotron x-ray diffraction experiments were performed by using a four-circle diffractometer on BL-3A and 4C at Photon Factory, KEK, Japan. The photon energy of the incident x-ray was tuned to 9.5 keV. The sample was mounted in a He closed-cycle refrigerator. Symmetry lowering was monitored by the emergence of superlattice reflection (0 −1/2 3/2) and forbidden reflection (1 0 2). The lattice spacing $1/c^*$ was estimated from the peak position of (0 0 2) reflection. In the measurement of x-ray-induced phase transition, the incident x-ray photon flux was monitored by a photodiode.

III. STRUCTURAL PHASE DIAGRAM

Figure 2 shows temperature dependence of the profiles of (0 −1/2 3/2) and (1 0 2) reflections in $V_{1-x}W_xO_2$ films with various x values. For $x \leqslant 0.07$, the reflections appear at low temperatures, indicating that V ions are dimerized. In contrast, (0 −1/2 3/2) diffraction peak does not appear in the whole temperature range for $x = 0.11$, which suggests the absence of the V dimerization. Temperature dependence of the intensities of the superlattice and forbidden reflections is compared with that of resistivity and c-axis length in Fig. 3, and based on those data, a phase diagram is established in Fig. 4(a). As shown in Fig. 3(a), the electrical resistivity of undoped film changes by more than two orders of magnitude across the transition accompanied by a change in the c-axis length of about 0.3%. Simultaneously, (0 −1/2 3/2) and (1 0 2) reflections emerge. W doping of $x = 0.02$ reduces the metal-insulator transition temperature by more than 50 K. The change in resistivity is more gradual and smaller than the undoped film. Nevertheless,

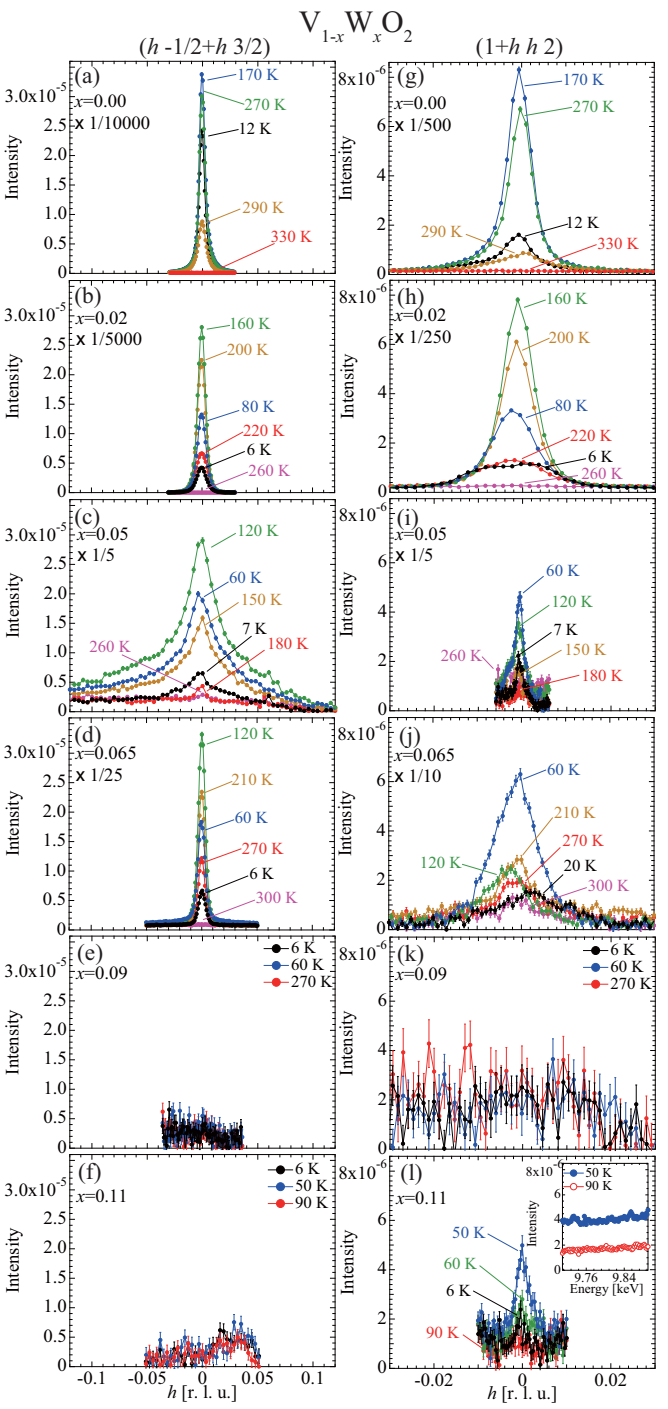

FIG. 2. (Color online) The temperature dependence of the peak profiles of superlattice (0 −1/2 3/2) and forbidden (1 0 2) reflections is shown for (a, g) $x = 0.00$, (b, h) $x = 0.02$, (c, i) $x = 0.05$, (d, j) $x = 0.065$, (e, k) $x = 0.09$, and (f, l) $x = 0.11$. The profiles along [1 1 0]-reciprocal-lattice-direction are measured at each temperature. The inset of panel (l) is the photon-energy dependence of (1 0 2) reflection measured at 50 K (larger-x-insulating phase) and 90 K (metallic phase).

the increase in the c-axis length is enhanced, as shown in Fig. 4(b). The superlattice and forbidden reflection peaks are slightly broader and weaker than at $x = 0$ [Figs. 4(c) and 4(d)], while the behavior essentially remains the same.

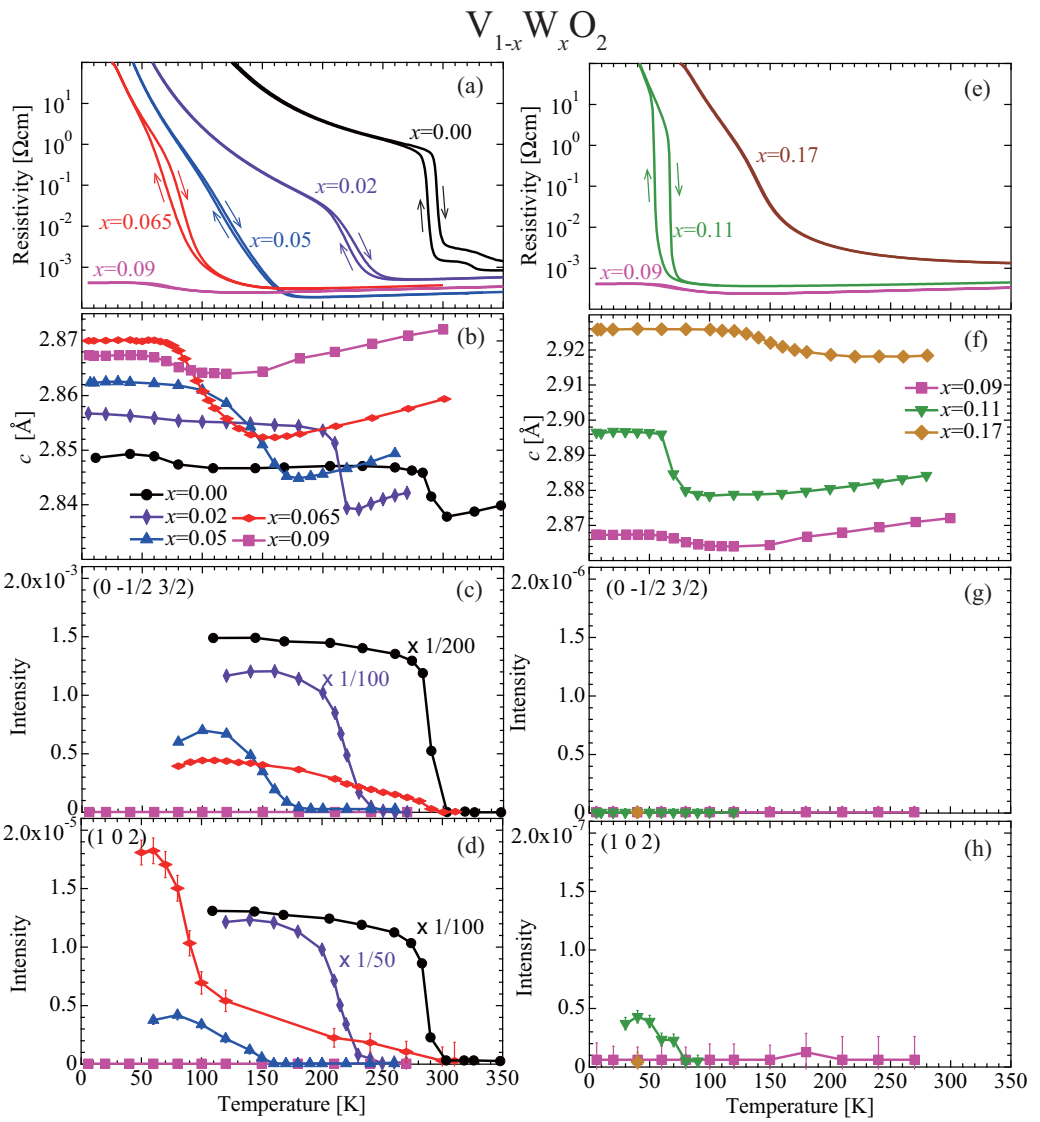

FIG. 3. (Color online) Temperature dependence of (a, e) resistivity, (b, f) c-axis length, (c, g) the intensity of superlattice (0 $-1/2$ 3/2), and (d, h) forbidden (1 0 2) reflections for $x = 0.00$, 0.02, 0.05, 0.065, 0.09, 0.11, and 0.17. The intensities are normalized by that of (0 0 2) reflection.

It is noteworthy that the modulation vector of V-dimerization also remains to be commensurate (0 1/2 1/2). This result would contradict a naive picture of Peierls-type metal-insulator phenomenon, where the wave vector is correlated with the value of Fermi wave number $\boldsymbol{k}_{\mathrm{F}}$.

By increasing the W concentration to $x = 0.05$, the temperature dependence of the c-axis length as well as resistivity change across the metal-insulator transition becomes more gradual. The superlattice and the forbidden reflections lose their intensity by two orders of magnitude. The full width at half maximum of the superlattice reflection is as broad as 0.04 reciprocal lattice units. These results imply that the density of V dimers should decrease to 1/10 or less, and the coherent region should be limited within 25 units. This estimation casts doubt on the scenario that the V dimerization plays the main role in the metal-insulator phase transition, because the transition temperature in $x = 0.05$ decreases only by a factor of $\sim$1/2 compared with the undoped case.

Moreover, for $x = 0.065$, the cell doubling and the monoclinic distortion appear just below room temperature, which is far above the metal-insulator transition temperature at $\sim$150 K, below which the c-axis length also begins to increase, as shown in Figs. 3(c) and 3(d). The peak width of (0 $-1/2$ 3/2) reflection of $x = 0.065$ is sharper than that of $x =$ 0.05, which conflicts with a simple expectation of dilution of V dimers by W substitution. Similar behaviors are also observed in other samples of almost the same compositions (see Supplemental Material [29]). The intensity maps of (0 $-1/2$ 3/2) reflection for $x = 0.065$ in the K-L reciprocal lattice plane at 100 K [Fig. 5(c)] and 200 K [Fig. 5(d)] show a temperature-independent peak position in both the insulating and metallic phases. The temperature dependence of the c-axis length and the intensity of the (0 $-1/2$ 3/2) reflection for $x =$ 0.065 is not affected by the irradiation of $\sim 10^{16}$ photon/cm^2 x-ray above $\sim$70 K, as shown in Figs. 5(a) and 5(b). Since all these data cannot be explained by phase separation, we

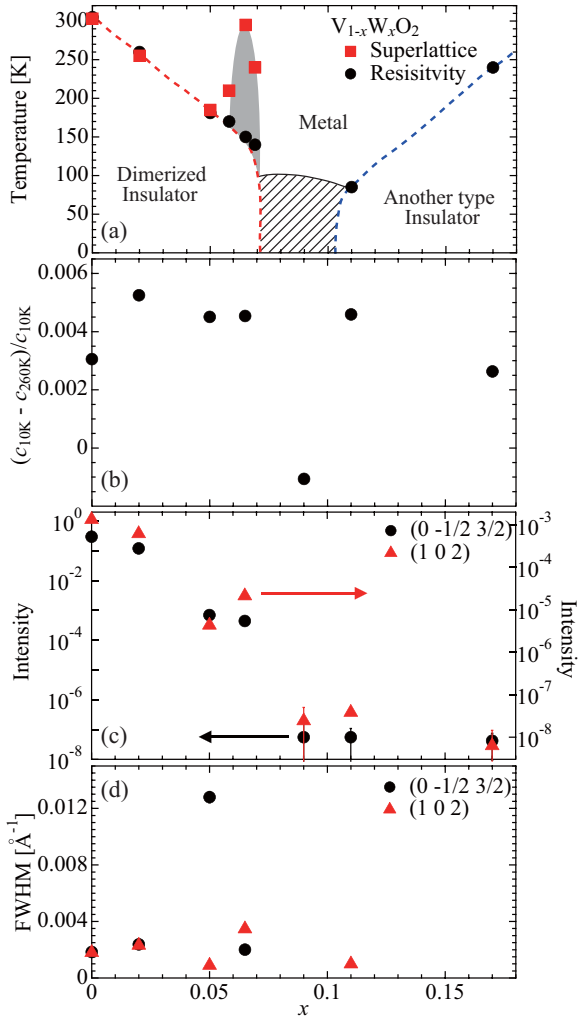

FIG. 4. (Color online) (a) Phase diagram determined from the temperature dependence of the resistivity and superlattice reflection. Filled circles (squares) represent the transition temperature determined from the resistivity (superlattice reflection), respectively. Gray area shows the metallic dimer phase. Hatched area indicates the tetragonal metallic phase coexisting with a small amount of the insulating phase. (b) The W-content dependence of normalized change of c-axis length from 260 K to 10 K. At $x = 0.00$, the data at 350 K is used instead of that at 260 K, because the metal-insulator transition temperature is higher than 260 K. (c, d) W-content dependence of (c) normalized intensities and (d) peak width of superlattice (0 $-1/2$ 3/2) and forbidden (1 0 2) reflections. The intensities and peak widths of each x-component are respectively measured at 110 K for $x = 0.00$, 160 K for $x = 0.02$, 100 K for $x = 0.05$, 0.065, and 0.09, and 40 K for $x = 0.11$ and 0.17, at which strongest intensity is observed. All intensities are normalized by that of (0 0 2) reflection for each composition.

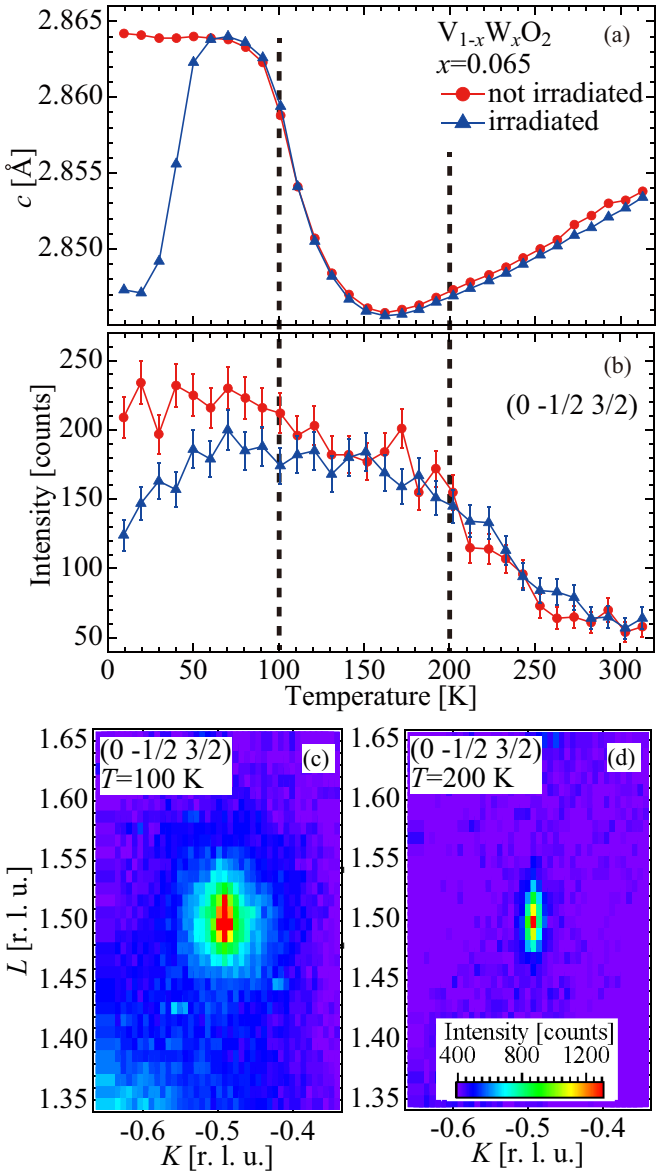

FIG. 5. (Color online) Temperature dependence of (a) c-axis length and (b) the peak intensity of a superlattice (0 $-1/2$ 3/2) reflection before (circles) and after (triangles) an irradiation of about 10^{16} cm^{-2} x-ray photons for $x = 0.065$ film. (c, d) Contour plots in the reciprocal plane of (0 K L) for (0 $-1/2$ 3/2) superlattice reflection at (c) 100 K and (d) 200 K.

conclude that a metallic phase with a cell-doubled structure (metallic dimer phase) exists in this composition. The metallic phase with the cell-doubling is observed in the region as shown with gray color in Fig. 4(a).

As shown in Figs. 3(e) and 3(f), for $x = 0.11$, a first-order metal-insulator transition with a change of the c-axis length is observed between 50 and 80 K. The transition temperature increases with increasing x to 0.17. The transition becomes gradual and the positive temperature-slope of resistivity is not observed even above the transition temperature. This semiconductor-like behavior can be attributed to the disorder induced by W doping [21]. The (0 $-1/2$ 3/2) reflection is not observed in the $x = 0.11$ sample, while the (1 0 2) reflection is observed, as shown in Figs. 2(f), 2(l), 3(g), and 3(h). The peak width of (1 0 2) reflection for $x = 0.11$ is comparable with that of an undoped film. We also observed (0 0 3) reflection, which does not satisfy the reflection condition of the rutile structure. The (1 0 2) and (0 0 3) reflections observed for $x = 0.11$ may not be assigned to multiple scatterings, because the peak-top intensity is almost independent of photon energy, as shown in

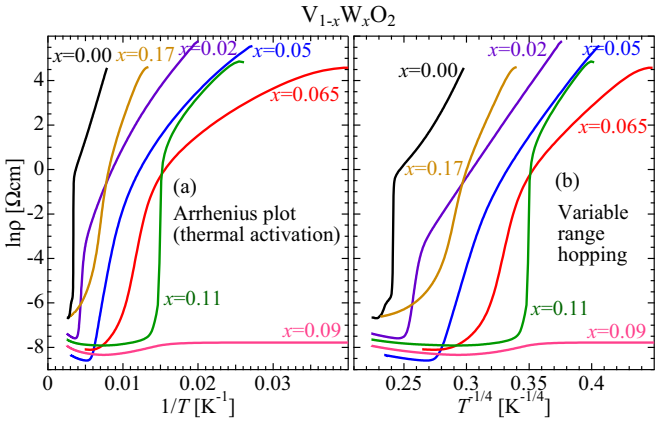

FIG. 6. (Color online) The $\ln\rho$ versus (a) T^{-1} and (b) $T^{-1/4}$ dependence for $V_{1-x}W_xO_2$ thin films, which correspond to a thermal-activation-type and a three-dimensional variable range hopping conduction, respectively.

the inset of Fig. 2(l). A plausible crystal structure of the low-temperature insulating phase is monoclinic phase with $P2/m$ space group as previously suggested in Cr-doped VO_2 [30]. These results suggest that the metal-insulator and structural phase transitions without V dimerization simultaneously take place for $x \geqslant 0.11$, while the space groups of $x = 0.11$ and 0.17 are not uniquely determined yet. For instance, neither (1 0 2) nor (0 0 3) reflection is observed in the insulating phase for $x = 0.17$, in contrast to the increase of the metal-insulator transition temperature with the expansion of the c axis. Further studies are necessary to pin down the precise crystal structures.

Next we discuss the origin of the metal-insulator transition. The insulating phase for $x \leqslant 0.07$ always accompanies the doubling of the unit cell. This would open an energy gap at $k_z = \pm\pi/2c$ in the quasi-one-dimensional band. However, this gap alone cannot turn the W-doped film into a band (Peierls) insulator, because the electron number deviates from the half filling. The steep decrease in the intensity of the superlattice reflections [Fig. 4(c)] with W doping seems to be inconsistent with the gradual change in the metal-insulator transition temperature. Nevertheless, the V dimerization still plays an important role in the metal-insulator transition for $x \leqslant 0.05$. For $x \sim 0.065$, the onset of the cell doubling does not coincide with the metal-insulator transition temperature, as shown in Fig. 4(a). This may cast a strong doubt on the Peierls model. Figure 6 shows temperature dependence of resistivity for various x values. While the temperature dependence of resistivity of the insulating phase in the undoped film can be fitted to the thermal activation of carriers, the doped film does not obey the activation law, as shown in Fig. 6(a). The resistivity curves seem to be better fitted to the variable range hopping model [Fig. 6(b)] [31]. The c-axis length shows a change upon the metal-insulator transition irrespective of W concentration x. The elongated c axis may reduce the bandwidth of the conduction band, cooperatively with the cell doubling. The decrease in the bandwidth can trigger a Mott-Anderson transition as affected by a random Coulomb potential induced by the W^{6+} substitution for V^{4+} ion. For $x \geqslant 0.11$, the superlattice reflection is not observed. When the formal valence of V ion is close to 4+ ($3d^1$), V ions are partially dimerized to form a spin singlet local bond, which would assist the localization. When the V valence largely deviates from 4+, the long-range order of the V dimers is no more observed. The metal-insulator transition is yet correlated with a change in the c-axis length. The resistivity curve is again explained in terms of the variable range hopping of carriers. Thus, we propose that the carriers of W-doped VO_2 are localized by the combined effect of the random potential of W^{6+} ions and the narrowing of the bandwidth accompanied by the elongated c axis. A recent report proposed a structural instability in the VO_2 material. The present W-doped VO_2 system may exhibit the metal-insulator transition by the cooperative mechanism of the crystal and electronic structural transition [32]. Further theoretical and experimental studies are necessary to clarify this issue.

The resistivity of the $x = 0.09$ sample saturates at low temperatures, as shown in Fig. 3(a). Figures 2(e) and 2(k) show that the (0 −1/2 3/2) and (1 0 2) reflections are not observed at any temperature. These results indicate that a metallic state for $x = 0.09$ retains the tetragonal structure down to the lowest temperature. This metallic phase intervenes between the two insulating phases which locate at low temperatures for the smaller-x and the larger-x ranges. Weak anomalies observed in resistivity and c-axis length around 70 K [see Figs. 3(a) and 3(b)] may be attributed to a small amount of contamination of neighboring insulating phases, as reported in Ref. [21].

IV. X-RAY-INDUCED PERSISTENT PHASE TRANSITION

We have investigated in detail the x-ray-induced phase transition in W-doped VO_2 thin films. Figures 7(a)–7(f) show the temperature dependence of the c-axis lengths and diffraction profiles of (0 0 2) reflection before and after the irradiation of $\sim 10^{16}$ photon/cm^2 x-ray beam at 7 K for $x = 0.05$, 0.065, and 0.11. For $x = 0.065$, a persistent shrinkage of the c-axis length induced by the irradiation of x-ray is observed below 40 K [see Figs. 7(b) and 7(e)], which is consistent with the result reported in Ref. [26]. The integrated intensities of the simultaneously measured (0 −1/2 3/2) and (1 0 2) reflections also decrease at 7 K, indicating that the irradiated film changes to a nondimerized metallic state. Here it should be noted that x-ray with a fairly high flux was irradiated to the film for the measurements of (1 0 2) and (0 −1/2 3/2) reflections. The similar persistent phase transition is also observed for $x = 0.05$ and $x = 0.11$, as shown in Fig. 7, in which the intensities of the superlattice and forbidden reflections decrease. The shrinkage of the c-axis length is commonly observed, namely, the x-ray-induced phase transition generally takes place not only for $x \leqslant 0.07$ but also for $x \geqslant 0.11$.

Next we discuss the transient states of crystal lattice during the x-ray-induced phase transition. Figure 8(a) shows the time evolution of the profile of (0 0 2) reflection for $x = 0.065$. The observed peak position of (0 0 2) reflection of the $x = 0.065$ film is 0.697 Å^{-1} and 0.701 Å^{-1} at 0 s before and 2000 s after starting the irradiation of x-ray, respectively. The peak gradually shifts to higher q^* values with longer exposure to the x-ray irradiation. After 100-s irradiation of x-ray, the peak of (0 0 2) reflection shifted to an intermediate position. Broadening of the peak observed in the transient state implies a nanoscale phase separation of the smaller-x insulator and

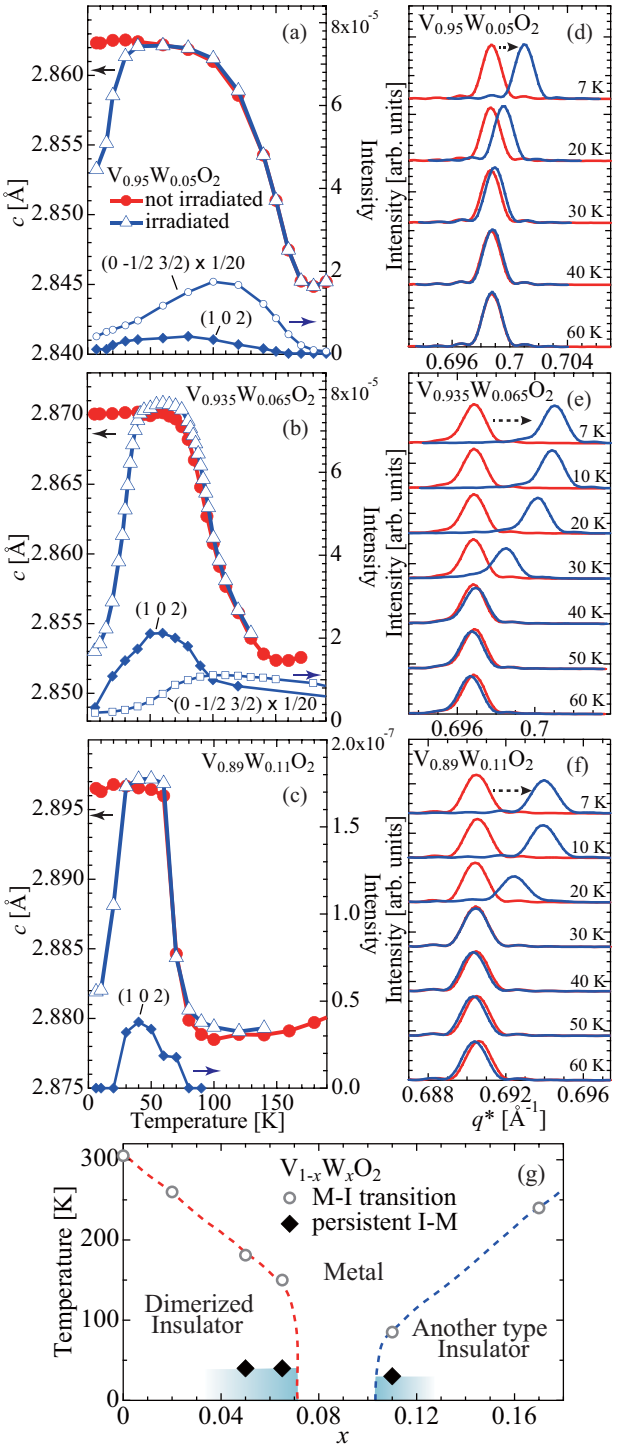

FIG. 7. (Color online) Temperature dependence of c-axis length, superlattice (0 −1/2 3/2), forbidden (1 0 2), and peak profile of (0 0 2) reflection for (a, d) $x = 0.05$, (b, f) 0.065, and (c, f) 0.11 before and after irradiation of strong x-ray and subsequent x-ray-induced phase transition. The decreases in intensity of superlattice and forbidden reflections at low temperatures is ascribed to the x-ray-induced phase transition. (g) X-ray-induced persistent phase transition is observed in the shaded regions. The open circles and solid diamonds represent the metal-insulator transition temperature and the boundaries for the persistent phase transition, respectively.

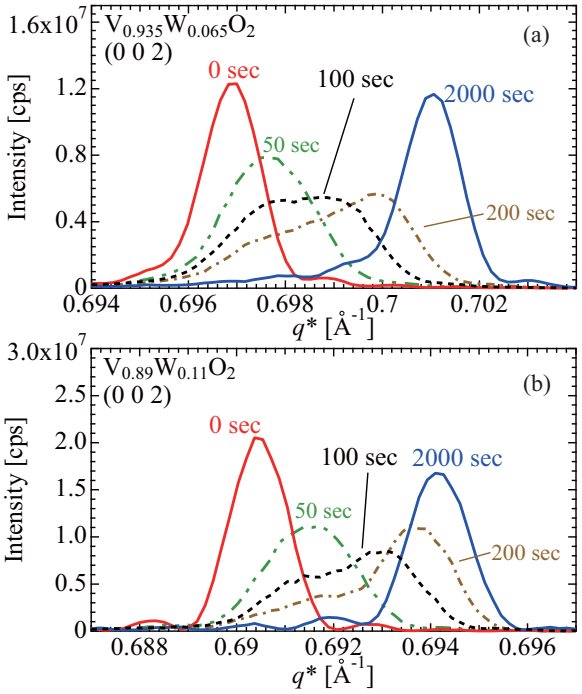

FIG. 8. (Color online) X-ray irradiation time dependence of the peak profile of (0 0 2) reflections for (a) $x = 0.065$ and (b) 0.11. Observed peak profile of the transient state for $x = 0.11$ is similar to that of $x = 0.065$. The irradiation time of strong incident x-ray are indicated for respective peak profiles.

metallic phases, as was pointed out in Ref. [26]. The evolution of the profile of (0 0 2) reflection for $x = 0.11$ is shown in Fig. 8(b). The peak moves from 0.6905 Å^{-1} to 0.694 Å^{-1} after 2000-s x-ray irradiation. The peak profile after 100-s x-ray irradiation of $x = 0.11$ is similar to the case of $x = 0.065$. Nanometer-size domains of insulating and metallic phases should coexist in the transient state. The similarity of the transient states for $x = 0.065$ and $x = 0.11$ suggests that the competition of two phases should play a major role in the x-ray-induced persistent phase transition, irrelevant to the detail of the electronic structures.

Irradiated x-ray photon number (n) dependence of the diffraction intensity at the (0 0 2) peak position of the insulating phase was measured at 7 K. In the samples of $x = 0.05$, 0.065, and 0.11, the intensity steeply decreases with the x-ray irradiation, as shown in Fig. 9. This decay process is explained by a simple model. We divide the crystal lattice into segments and assume that an x-ray photon should convert an insulating segment into metallic with a probability p. The evolution of the number N_I of insulating segments by x-ray irradiation obeys $\Delta N_I/\Delta n = -N_I p$. Since the diffraction intensity I is proportional to N_I in the first approximation, I is expressed as $I = I_0 \exp(-pn)$. Here I_0 indicates the intensity before x-ray irradiation. The probability p for $x = 0.05$, 0.065, and $x = 0.11$ are estimated to be 0.56×10^{-15} cm^2, 5.51×10^{-15} cm^2, and 5.27×10^{-15} cm^2, respectively. The necessary photon number for x-ray-induced phase transition is small in the vicinity of the metal-insulator phase boundary and increases as x goes away from the

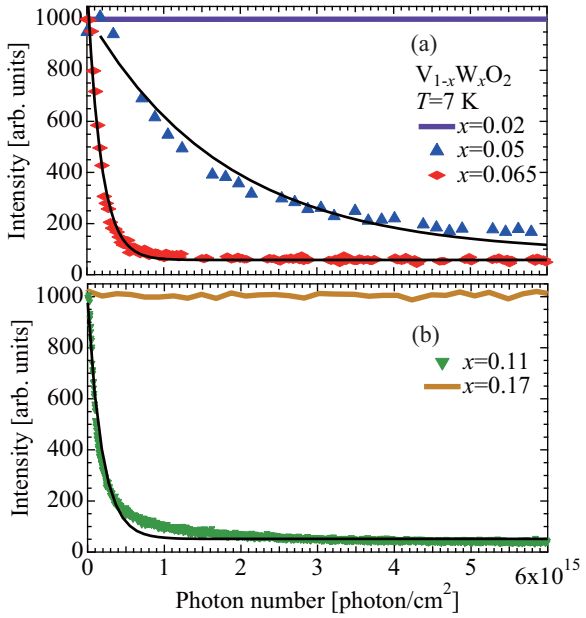

FIG. 9. (Color online) Irradiated x-ray photon number dependence of the peak-top intensity at the insulating (0 0 2) position in (a) the smaller-x and (b) the larger-x insulating phases. The obtained data are fitted by using the function of $I = I_0 \exp(-pn) + I_b$. I, I_0, p, n, and I_b indicate the observed intensity, the intensity before x-ray irradiation, the probability to convert an insulating segment into metallic by an x-ray photon, the irradiated photon number, and the background intensity, respectively.

boundary. For $x = 0.02$ and 0.17, x-ray irradiation effect is not observed up to 10^{19} photon/cm^2.

The x-ray-induced persistent phase transition is observed only at low temperatures, as shown in Fig. 7(g). Even at the lowest temperature the c-axis length after the irradiation is not as short as that of the metallic phase, as shown in Figs. 7(a)–7(c). This suggests that small regions of the insulating phase coexist with the metallic phase even after an irradiation of many x-ray photons. The c-axis length gradually increases as the temperature goes up and becomes identical to that of the insulating phase above 30 ∼ 40 K. The volume ratio of the insulating phase gradually approaches 100%. Here a double-peak structure does not appear in the warming process. This implies that both phases should be distributed in a tiny spatial scale (possibly ∼nm). The local transition is similar to that in the thermoluminescence and color-center formation by x-ray irradiation in alkali halides ionic crystal, in which the absorbed x-ray excites the core electron, giving rise to the local defect of the core hole [33–37].

V. SUMMARY

We have performed synchrotron x-ray diffraction measurements to investigate the structural aspects of the thermally and x-ray-induced metal-insulator phase transitions in W-doped VO_2 thin films. V-dimerization-type distortion is only observed in the insulating phase for $x \leqslant 0.07$. On the other hand, the c axis is found to expand in both the insulating phases, which may decrease the electronic band width. Temperature dependence of resistivity suggests that Mott-Anderson mechanism should play an important role in both the insulating phases. The x-ray-induced persistent phase transition is observed below 30 ∼ 40 K in the vicinity of the boundary between metal and each insulating phase. An absorbed x-ray photon creates a small cluster of metallic phase. The size of the cluster becomes smaller in the film in the deeply insulating phase distant from the phase boundary. With increasing the irradiated photon number, the volume of the metallic phase shows a saturation.

ACKNOWLEDGMENTS

The authors are grateful to Y. Kitagawa, Y. Wakabayashi, M. Nakamura, K. Kobayashi, J. Okamoto, and Y. Tokunaga for fruitful discussions. The synchrotron x-ray diffraction experiments were performed with the approval of the Photon Factory Program Advisory Committee (Grants No. 2009S2-003 and No. 2012G649). This work was supported in part by Funding Program for World-Leading Innovative R&D on Science and Technology (FIRST Program) from the JSPS and Grants-in-Aid for scientific research (Grants No. 24224009 and No. 24226002), and from MEXT, Japan.

[1] N. F. Mott, Rev. Mod. Phys. **40**, 677 (1968).
[2] M. Imada, A. Fujimori, and Y. Tokura, Rev. Mod. Phys. **70**, 1039 (1998).
[3] F. J. Morin, Phys. Rev. Lett. **3**, 34 (1959).
[4] G. Andersson, Acta Chem. Scand. **10**, 623 (1956).
[5] S. Biermann, A. Poteryaev, A. I. Lichtenstein, and A. Georges, Phys. Rev. Lett. **94**, 026404 (2005).
[6] J. H. Park, J. M. Coy, T. S. Kasirga, C. Huang, Z. Fei, S. Hunter, and D. H. Cobden, Nature **500**, 431 (2013).
[7] J. B. Goodenough, J. Solid State Chem. **3**, 490 (1971).
[8] S. Shin, S. Suga, M. Taniguchi, M. Fujisawa, H. Kanzaki, A. Fujimori, H. Daimon, Y. Ueda, K. Kosuge, and S. Kachi, Phys. Rev. B **41**, 4993 (1990).
[9] R. M. Wentzcovitch, W. W. Schulz, and P. B. Allen, Phys. Rev. Lett. **72**, 3389 (1994).
[10] T. M. Rice, H. Launois, and J. P. Pouget, Phys. Rev. Lett. **73**, 3042 (1994).
[11] M. W. Haverkort, Z. Hu, A. Tanaka, W. Reichelt, S. V. Streltsov, M. A. Korotin, V. I. Anisimov, H. H. Hsieh, H.-J. Lin, C. T. Chen, D. I. Khomskii, and L. H. Tjeng, Phys. Rev. Lett. **95**, 196404 (2005).
[12] J. M. Tomczak, F. Aryasetiawan, and S. Biermann, Phys. Rev. B **78**, 115103 (2008).
[13] M. Marezio, D. B. McWhan, J. P. Remeika, and P. D. Dernier, Phys. Rev. B **5**, 2541 (1972).
[14] J. P. Pouget, H. Launois, T. M. Rice, P. Dernier, A. Gossard, G. Villeneuve, and P. Hagenmuller, Phys. Rev. B **10**, 1801 (1974).
[15] G. Villeneuve, A. Bordet, A. Casalo, J. P. Pouget, H. Launois, and P. Lederer, J. Phys. Chem. Solids **33**, 1953 (1972).
[16] T. Horlin, T. Niklewski, and M. Nygren, Mater. Res. Bull. **7**, 1515 (1972).
[17] T. Horlin, T. Niklewski, and M. Nygren, Mater. Res. Bull. **8**, 179 (1973).

[18] K. L. Holman, T. M. McQueen, A. J. Williams, T. Klimczuk, P. W. Stephens, H. W. Zandbergen, Q. Xu, F. Ronning, and R. J. Cava, Phys. Rev. B **79**, 245114 (2009).
[19] C. Tang, P. Georgopoulos, M. E. Fine, J. B. Cohen, M. Nygren, G. S. Knapp, and A. Aldred, Phys. Rev. B **31**, 1000 (1985).
[20] A. Romanyuk, R. Steiner, L. Marot, and P. Oelhafen, Sol. Energy Mater. **91**, 1831 (2007).
[21] K. Shibuya, M. Kawasaki, and Y. Tokura, Appl. Phys. Lett. **96**, 022102 (2010).
[22] J. S. Lee, K. Shibuya, M. Kawasaki, and Y. Tokura, Phys. Rev. B **85**, 155110 (2012).
[23] E. Sakai, K. Yoshimatsu, K. Shibuya, H. Kumigashira, E. Ikenaga, M. Kawasaki, Y. Tokura, and M. Oshima, Phys. Rev. B **84**, 195132 (2011).
[24] A. Cavalleri, Cs. Tóth, C. W. Siders, J. A. Squier, F. Ráksi, P. Forget, and J. C. Kieffer, Phys. Rev. Lett. **87**, 237401 (2001).
[25] A. Cavalleri, M. Rini, H. H. W. Chong, S. Fourmaux, T. E. Glover, P. A. Heimann, J. C. Kieffer, and R. W. Schoenlein, Phys. Rev. Lett. **95**, 067405 (2005).
[26] K. Shibuya, D. Okuyama, R. Kumai, Y. Yamasaki, H. Nakao, Y. Murakami, Y. Taguchi, T. Arima, M. Kawasaki, and Y. Tokura, Phys. Rev. B **84**, 165108 (2011).
[27] Y. Tokura, Rep. Prog. Phys. **69**, 797 (2006).
[28] V. Kiryukhin, D. Casa, J. P. Hill, B. Keimer, A. Vigliante, Y. Tomioka, and Y. Tokura, Nature **386**, 813 (1997).
[29] See Supplemental Material at http://link.aps.org/supplemental/10.1103/PhysRevB.91.064101 for the transition temperatures of the other samples.
[30] J. B. Goodenough and H. Y.-P. Hong, Phys. Rev. B **8**, 1323 (1973).
[31] N. F. Mott, Phil. Mag. **19**, 835 (1969).
[32] Z. Hiroi, H. Hayamizu, T. Yoshida, Y. Muraoka, Y. Okamoto, J. Yamaura, and Y. Ueda, Chem. Mater. **25**, 2202 (2013).
[33] F. Seitz, Rev. Mod. Phys. **18**, 384 (1946); **26**, 7 (1954).
[34] R. W. Christy and W. E. Harte, Phys. Rev. **109**, 710 (1958).
[35] H. Rabin, Phys. Rev. **116**, 1381 (1959).
[36] S. Mascarenhas, D. A. Wiegand, and R. Smoluchowski, Phys. Rev. **134**, A481 (1964).
[37] H. N. Hersh, Phys. Rev. **148**, 928 (1966).